Dehydration Behavior of Synthetic $Al_{0.5}Fe_{0.5}PO_4 \cdot 2.5H_2O$

Banjong Boonchom*[,†,‡] and Naratip Vittayakorn[‡,§,||]

King Mongkut's Institute of Technology Ladkrabang, Chumphon Campus, 17/1 M. 6 Pha Thiew District, Chumphon, 86160, Thailand, Advanced Materials Science Research Unit, Department of Chemistry, Faculty of Science, King Mongkut's Institute of Technology Ladkrabang, Bangkok 10520, Thailand, Electroceramic Research Laboratory, College of KMITL Nanotechnology, King Mongkut's Institute of Technology Ladkrabang, Bangkok 10520, Thailand, and ThEP Center, CHE, 328 Si Ayutthaya Rd., Bangkok 10400, Thailand

The dehydration behavior of the experimentally produced $Al_{0.5}Fe_{0.5}PO_4 \cdot 2.5H_2O$ solid solution is assessed from thermogravimetrical (TG, differential thermogravimetric, DTG, and differential thermal analysis, DTA) and differential scanning calorimetry (DSC) analyses. The dehydration proceeded through a well-defined step at low temperatures (< 300 °C), which corresponds to the loss of 2.5 water molecules. The fluctuating dependence of the activation energies on fraction mass loss (α) for the dehydration reaction of $Al_{0.5}Fe_{0.5}PO_4 \cdot 2.5H_2O$ calculated through isoconversional methods (Ozawa and the Kissinger−Akahira−Sunose) indicates the existence of a complex multistep mechanism. The Avrami exponent value of 1.11 is indicative of one-dimensional growth as a phase boundary mechanism. The thermodynamic functions (ΔH^*, ΔG^*, and ΔS^*) of the dehydration reaction calculated from the DSC technique are discussed for the first time.

1. Introduction

Iron phosphate $FePO_4 \cdot 2H_2O$ and aluminum phosphate $AlPO_4 \cdot 2H_2O$ are minerals and synthesized phosphate materials with similar structures (isostructural). The existence of several crystalline $FePO_4 \cdot 2H_2O$ and $AlPO_4 \cdot 2H_2O$ phases has been reported in the literature.[1−3] $FePO_4 \cdot 2H_2O$ phases include strengite and metastrengite, whereas $AlPO_4 \cdot 2H_2O$ phases include variscite and metavariscite. Strengite and variscite are orthorhombic systems, *Pcab*, whereas metastrengite and metavariscite are monoclinic systems, *C*2/*m*. They are interesting in both environmental and technological fields such as catalysts, wastewater purification systems, ferroelectrics, lithium batteries, and the steel and glass industries.[4−7] With reference to the former, the formation of Fe- and Al-PO_4 compounds helps remove phosphate from wastewaters, or in other instances, their dissolution helps regulate the release of phosphate and Fe in acid soils.[1−3] In terms of technological relevance, Fe- and Al-PO_4 materials are important in the area of catalysis and electrochemical cells, due to their surface acidity and thermal and chemical stabilities.[7−10] It is known that, to some extent, Fe(III) and Al(III) cations can substitute for each other within the structure of these materials. Moreover, there exists a stoichiometric mineral known as $Al_{0.5}Fe_{0.5}PO_4 \cdot nH_2O$, in which both cations are in a 1:1 proportion.[11] The Fe- and Al-phosphate solid solution is of interest because the varying composition of metal cations can change their useful properties such as a catalyst for organic syntheses[11,12] and electrochemical cells for lithium batteries.[6,7]

The miscibility in the Fe- and $AlPO_4$ system as well as the dehydration behavior of both $FePO_4 \cdot 2H_2O$ and $AlPO_4 \cdot 2H_2O$ has been the subject of intense scientific research.[13,14] The thermal treatment of iron aluminum phosphate hydrate ($Al_{0.5}Fe_{0.5}PO_4 \cdot nH_2O$; $n = 1.8$ to 2.5) relating to the dehydration reaction at high temperatures has a great synthetic potential, as it may turn a simple compound into an advanced material ($Al_{0.5}Fe_{0.5}PO_4$). The losses of constitutional and crystallization water of a solid during thermal treatment influence dispersity, layer thickness, specific area, porosity, shape, and size of the material,[1−4] which are useful physical properties for specific applications.[13,14] Thermogravimetry is a universal technique widely used for the measurement of kinetic and thermodynamic parameters of dehydration and/or decomposition reactions, which involve physical changes and chemical reactions in the fields of industrial and scientific research.[15,16] However, the mixing properties and the dehydration behavior of the $Al_{0.5}Fe_{0.5}PO_4 \cdot nH_2O$ solid solution have not been studied. Herein, the present work includes the mechanism, kinetics, and thermodynamics associated with the transition from $Al_{0.5}Fe_{0.5}PO_4 \cdot 2.5H_2O$ to $Al_{0.5}Fe_{0.5}PO_4$ phases using TG-DTG-DTA (thermogravimetry, differential thermogravimetry, differential thermal analysis) and DSC (differential scanning calorimetry). The obtained data play an important role in the theoretical study, application development, and industrial production of the compound as a basis of theoretical analysis and will be important for further studies of this compound.

2. Experimental Section

2.1. Sample Synthesis. $Al_{0.5}Fe_{0.5}PO_4 \cdot 2.5H_2O$ powder was synthesized by mixing the solutions of 0.1 M $FeCl_3 \cdot 6H_2O$, 0.1 M $AlCl_3 \cdot 6H_2O$, and 0.2 M $NaH_2PO_4 \cdot H_2O$ with 2.0 M NaOH, following the coprecipitation method. Appropriate amounts of 0.1 M $FeCl_3 \cdot 6H_2O$ and 0.1 M $AlCl_3 \cdot 6H_2O$ were mixed in a beaker followed by adding an equivalent amount of 0.2 M $NaH_2PO_4 \cdot H_2O$ with magnetic stirring at 90 °C. Finally, the gel solution was obtained by adding 2.0 M NaOH until the solution

* Corresponding author. Tel.: +66-7750-6422 ext 4565. Fax: +66-7750-6410. E-mail address: kbbanjon@kmitl.ac.th.
† King Mongkut's Institute of Technology Ladkrabang, Chumphon Campus.
‡ Advanced Materials Science Research Unit, King Mongkut's Institute of Technology Ladkrabang, Bangkok.
§ Electroceramic Research Laboratory, King Mongkut's Institute of Technology Ladkrabang, Bangkok.
|| ThEP Center, CHE.

10.1021/je100096e
Published on Web 06/02/2010

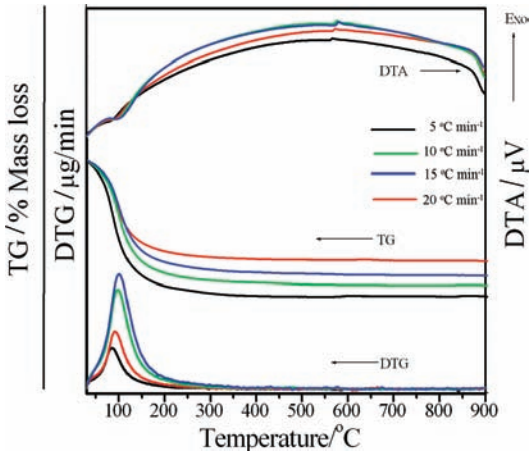

Figure 1. TG-DTG-DTA curves of $Al_{0.5}Fe_{0.5}PO_4 \cdot 2.5H_2O$ in dry air at heating rates of (5, 10, 15, and 20) °C·min^{-1}.

reaches pH 3.80. The precipitates were filtered by suction, washed by hot deionized water, and dried in air. The resultant solid was kept in a desiccator for further investigation.

2.2. Sample Characterization. Thermal analysis measurements of about (8.0 ± 0.3) mg sample mass were carried out by a Pyris1 Perkin-Elmer apparatus with an alumina crucible at heating rates of (5, 10, 15, and 20) °C·min^{-1} in dynamic air in the range of (30 to 900) °C. DSC was carried out for samples ((5 to 10) mg) in aluminum crucibles, over the temperature range of (50 to 500) °C using DSC, a Perkin-Elmer DSC 204 F1 Phoenix apparatus. The heating rate employed was 10 °C·min^{-1}. The structures of the prepared sample and its decomposed product were studied by X-ray powder diffraction using a D8 Advanced powder diffractometer (Bruker AXS, Karlsruhe, Germany) with Cu Kα radiation (λ = 0.1546 nm). The room temperature Fourier transform infrared (FTIR) spectra were recorded in the range of (4000 to 400) cm^{-1} with eight scans on a Perkin-Elmer Spectrum GX spectrometer with a resolution of 4 cm^{-1}. The morphology was examined by scanning electron microscopy (SEM) using Hitachi S4700 after gold coating.

3. Results and Discussion

3.1. Thermal Analysis. Figure 1 shows the TG-DTG-DTA curves of the thermal decomposition of $Al_{0.5}Fe_{0.5}PO_4 \cdot 2.5H_2O$ at four heating rates. TG curves of $Al_{0.5}Fe_{0.5}PO_4 \cdot 2.5H_2O$ show a single well-defined dehydration in the range of (30 to 300) °C. The water eliminated below 100 °C is related to the physical adsorbed water, whereas water eliminated at 100 °C and above (200 °C) can be considered as crystal water and coordinated water. The dehydration temperature obtained in this work suggest that the water in hydrated binary aluminum iron phosphate can be considered as physical adsorbed water and crystal water.[8,9,17,18] The peaks in the DTG and DTA curves closely correspond to the mass loss observed on the TG traces. All TG-DTG-DTA curves are approximately the same shape. However, the dehydration stage was shifted toward higher temperatures when the heating rates increase, which indicate that the mass loss is dependent on the heating rate. The average observed mass losses of four TG curves are 26.22 % by mass, which correspond to 2.51 mol of water, which is close to the theoretical value for $Al_{0.5}Fe_{0.5}PO_4 \cdot 2.5H_2O$ (26.11 %, 2.50 H_2O). An endothermic effect in the DTA curves is observed at about 100 °C that agrees with the respective DTG peak. Further, an exothermic effect at 572 °C without appreciable weight loss is observed in the DTA curve, which can be ascribed to a transition phase from an amorphous to crystalline form of $Al_{0.5}Fe_{0.5}PO_4$.[11]

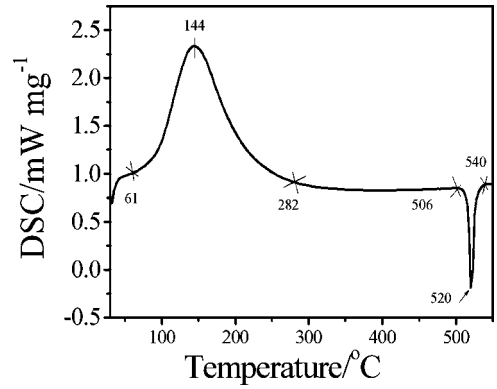

Figure 2. DSC curve of $Al_{0.5}Fe_{0.5}PO_4 \cdot 2.5H_2O$ at the heating rate of 10 K·min^{-1} in a N_2 atmosphere.

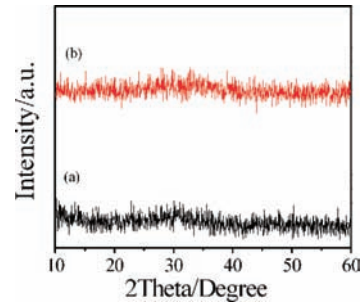

Figure 3. XRD patterns of $Al_{0.5}Fe_{0.5}PO_4 \cdot 2.5H_2O$ (a) and its decomposed product $Al_{0.5}Fe_{0.5}PO_4$ (b).

The retained mass of about 73.78 % is compatible with the value expected for the formation of $Al_{0.5}Fe_{0.5}PO_4$. The overall reaction is:

$$Al_{0.5}Fe_{0.5}PO_4 \cdot 2.5H_2O \rightarrow Al_{0.5}Fe_{0.5}PO_4 + 2.5H_2O \quad (1)$$

The binary iron aluminum phosphate, $Al_{0.5}Fe_{0.5}PO_4$, is found to be the final product of the thermal decomposition at $T > 300$ °C. The thermal stability, mechanism, and phase transition temperature of the synthesized $Al_{0.5}Fe_{0.5}PO_4 \cdot 2.5H_2O$ are lower than those of the dehydration reactions of individual metal phosphates ($AlPO_4 \cdot 2H_2O$[17] and $FePO_4 \cdot 2H_2O$[18]). On the basis of these results, we can conclude that the different thermal properties are caused by the incorporation of Fe and Al metals in the skeleton.

The DSC curve of $Al_{0.5}Fe_{0.5}PO_4 \cdot 2.5H_2O$ (Figure 2) shows an endothermic peak at 144 °C (onset peak at 61 °C) and an exothermic peak at 520 °C (onset peak at 506 °C) due to the dehydration and the transition phase from an amorphous to crystalline form of this compound, respectively. The temperatures of the DSC peaks are well in accordance with that of the DTG and DTA peaks (Figure 1), so results of the TG/DTG/DTA and DSC methods are credible.

3.2. XRD Analysis. The XRD studies of $Al_{0.5}Fe_{0.5}PO_4 \cdot 2.5H_2O$ and its dehydrated product $Al_{0.5}Fe_{0.5}PO_4$ revealed that the structures remained in the amorphous or poor crystallization phases as well as nanoparticles of these compounds (Figure 3). The problem here is that the XRD data show poorly crystalline patterns, which are no indication of $Al_{0.5}Fe_{0.5}PO_4 \cdot 2.5H_2O$ and $Al_{0.5}Fe_{0.5}PO_4$ as separated phases. The studied compounds synthesized by the precipitation route in this work were poor crystalline phases, which differ from crystallization phases of those synthesized by a hydrothermal method.[5−10] These results are in agreement with the results reported in the literature.[5−10]

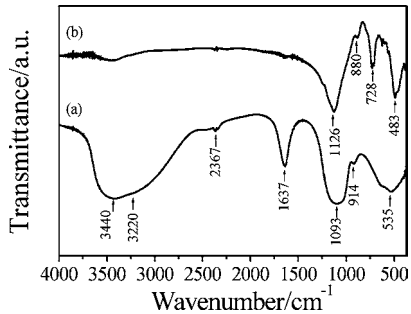

Figure 4. FTIR spectra of $Al_{0.5}Fe_{0.5}PO_4 \cdot 2.5H_2O$ (a) and its decomposed product $Al_{0.5}Fe_{0.5}PO_4$ (b).

3.3. FTIR Analysis. Figure 4 shows FTIR spectra of $Al_{0.5}Fe_{0.5}PO_4 \cdot 2.5H_2O$ and its dehydrated product $Al_{0.5}Fe_{0.5}PO_4$. The vibrational motions of $Al_{0.5}Fe_{0.5}PO_4 \cdot 2.5H_2O$ are divided into two block units of the water molecule H_2O and phosphate anion PO_4^{3-}, whereas $Al_{0.5}Fe_{0.5}PO_4$ is divided into a block unit of the only phosphate anion PO_4^{3-}. It is worth mentioning that the antisymmetric stretching (ν_{OH}), the symmetric stretching (ν_{OH}), and the bending (δ_{OH}) vibrations of water molecules are solely observed at (3440, 3220, and 1637) cm^{-1}, respectively. These bands disappear in the FTIR spectrum of $Al_{0.5}Fe_{0.5}PO_4$ (Figure 4b), implying the presence of anhydrous crystal. For the intramolecular vibrations of the PO_4^{3-} anion, we identify the symmetric stretching mode at $\nu_1 = 990$ cm^{-1}, the doublet at $\nu_2 =$ (447 to 485) cm^{-1}, the triplets ν_3 at (1000 to 1085) cm^{-1}, and the triplet ν_4 in the region (570 to 640) cm^{-1}. For condensed phosphates, the intensity of the P−O stretching IR bands near 1000 cm^{-1} are always greater than those near 880 cm^{-1}, assigned to the stretching vibration ν_{P-O-P} of P−O−P bridges. These phosphate band positions of $Al_{0.5}Fe_{0.5}PO_4 \cdot 2.5H_2O$ and $Al_{0.5}Fe_{0.5}PO_4$ are in excellent agreement with published data.[19,20]

3.4. SEM Analysis. The scanning electron micrographs of $Al_{0.5}Fe_{0.5}PO_4 \cdot 2.5H_2O$ (Figure 5a) and $Al_{0.5}Fe_{0.5}PO_4$ (Figure 5b) powders showed different uniform morphological features due to the loss of crystallization waters. It can be seen that the $Al_{0.5}Fe_{0.5}PO_4$ powders were clearly coarser than the $Al_{0.5}Fe_{0.5}PO_4 \cdot 2.5H_2O$ powders. The $Al_{0.5}Fe_{0.5}PO_4$ powders consisted of round particles near 100 nm in size along with a narrow size distribution Additionally, the SEM photographs show that both crystals have grown through a combination of surface deposition and agglomeration.

3.5. Kinetics Analysis. In the rate equation for the isothermal decomposition of a solid-state process,[21] A (solid) → B (solid) + C (gas) is often written from:

$$d\alpha/dt = A \exp(-E_a/RT) f(\alpha) \qquad (2)$$

In most thermal analysis experiments, the heating rate $\beta = dT/dt$ is a constant value, so eq 2 may also lead to the corresponding equations of Ozawa[22] and Kissinger−Akahira−Sunose (KAS)[23] methods after integration.

$$\text{Ozawa equation: } \ln \beta = \ln\left(\frac{AE_\alpha}{R\, g(\alpha)}\right) - 5.3305 - 1.0516\left(\frac{E_\alpha}{RT}\right) \qquad (3)$$

$$\text{KAS equation: } \ln\left(\frac{\beta}{T^2}\right) = \ln\left(\frac{AE_\alpha}{R\, g(\alpha)}\right) - \left(\frac{E_\alpha}{RT}\right) \qquad (4)$$

where A (the pre-exponential factor) and E_a (the activation energy) are the Arrhenius parameters and R is the gas constant.

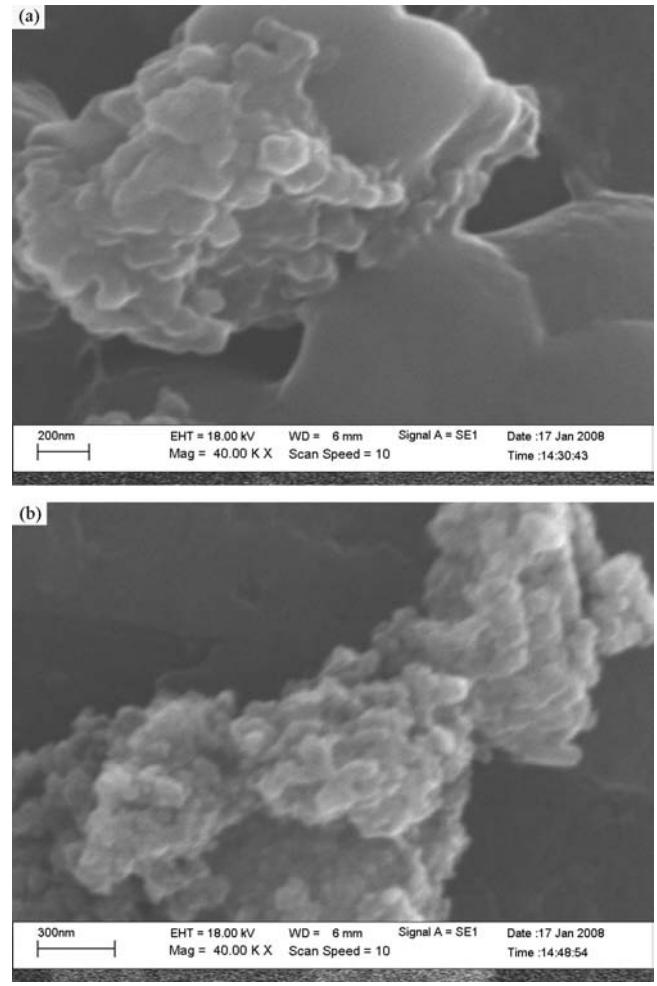

Figure 5. SEM photographs of $Al_{0.5}Fe_{0.5}PO_4 \cdot 2.5H_2O$ (a) and its decomposed product $Al_{0.5}Fe_{0.5}PO_4$ (b).

The $g(\alpha) = \int_0^\alpha (d\alpha/f(\alpha))$ is the integral form of $f(\alpha)$, which is the reaction model that depends on the reaction mechanism. The reaction can be expressed through the temperatures corresponding to fixed values of the extent of conversion ($\alpha = (m_i - m_a)/(m_i - m_f)$, where m_i, m_a, and m_f are the initial, actual, and final sample mass at time t) from experiments at different heating rates (β).

Hence, the dependences of ln β and ln β/T^2 on $1000/T$, calculated for the same α values (0.10 to 0.90) at different heating rates β ((5, 10, 15, and 20) °C·min^{-1}) can be used to calculate the activation energy, so we can obtain the activation energies through the experimental data for the dehydration of $Al_{0.5}Fe_{0.5}PO_4 \cdot 2.5H_2O$ as shown in Table 1. The activation energies E_α can be calculated from the slopes of the straight lines with a good coefficient of determination ($R^2 > 0.99$). The activation energies worked out through the Ozawa and the KAS methods vary slightly, so the results are credible. If E_α values are independent of α, the decomposition may be a simple reaction, while the dependence of E_α on α should be interpreted in terms of multistep reaction mechanisms.[24,25] From Table 1 it can be seen that the activation energies decrease first and increase at α higher than 0.6. A decreasing dependence of E_α on α is found for consecutive reactions, while an increasing dependence of E_α on α is found for competitive reactions. According to the decreasing E_α at $\alpha < 0.6$, the kinetics scheme of which corresponds to a reversible reaction followed by an irreversible one. In addition, the increasing E_α at $\alpha > 0.6$ corresponds to a two-pathway competitive reaction model.[24,25]

Table 1. Activation Energies (E_α) Versus the Coefficient of Detemination (R^2) Calculated by Ozawa and KAS Methods for the Dehydration of $Al_{0.5}Fe_{0.5}PO_4 \cdot 2.5H_2O$

	Ozawa method		KAS method	
α	E_α/kJ·mol^{-1}	R^2	E_α/kJ·mol^{-1}	R^2
0.1	231.14	0.9985	237.50	0.9985
0.2	158.58	0.9937	160.99	0.9933
0.3	136.83	0.9968	137.98	0.9965
0.4	129.85	0.9984	130.54	0.9983
0.5	126.05	0.9972	126.44	0.9970
0.6	125.90	0.9970	126.16	0.9966
0.7	136.37	0.9976	137.02	0.9974
0.8	167.18	0.9989	169.21	0.9988
0.9	275.09	0.9959	323.93	0.9957

So it is concluded that there is a fourth reaction for the dehydration reaction. Additionally, the obtained activation energy values of the dehydration reaction of the studied compound are higher than those of individual metal phosphates (69.68 ± 7 kJ·mol^{-1} (Kissinger method) for $AlPO_4 \cdot 2H_2O$[17] and 68.48 ± 1 kJ·mol^{-1} (Flynn−Wall−Ozawa method) and 65.55 ± 1 kJ·mol^{-1} (KAS method) for $FePO_4 \cdot 2H_2O$[18] reported in our previous works. As can be clearly seen, there is a direct relationship between the cation radius of Al(III) and Fe(III) and its thermal stability and activation energy of the dehydration reaction. A common conclusion is that the reason for this is the different interaction of iron and aluminum with water molecules in the structure, which supports the incorporation of Fe and Al metals in the skeleton and forms the $Al_{0.5}Fe_{0.5}PO_4 \cdot 2.5H_2O$ solid solution.

The Arvami exponent, *n*, can be evaluated by the Ozawa equation. First, the volume fraction of phase transition *x*, at the same temperature, *T*, from four crystallization steps under different heating rates is calculated by the ratio of partial area at *T* to the total area of crystallization. After plotting $\ln[-\ln(1 - x)]_T$ versus $\ln(\beta)$ and if the data can be fitted to the linear function, then the slope of the function is $-n$,[26] which is really the combined process of nucleation and growth. The most common approach used to describe the overall nonisothermal crystallization is given below:

$$-n = \frac{\mathrm{d}\ln[-\ln(1 - x)]}{\mathrm{d}\ln(\beta)} \tag{5}$$

The volumetric function of the growth mechanism directly affects the transformation rate, and the dimensionality of the transformation is reflected in the value of the Avrami exponent.[26,27] Higher dimensionality leads to a higher value of the exponent. Therefore, determination of the Avrami exponent allows one to determine which geometric model of the phase transformation is the best fit: one-, two-, or three-dimensional growth. For the dehydration step of $Al_{0.5}Fe_{0.5}PO_4 \cdot 2.5H_2O$, the Avrami exponent, *n*, has a value of 1.11 ($R^2 = 0.991$), indicating a one-dimensional growth mechanism. The Avrami exponent, in addition to giving information regarding the dimensionality of the growth, can also yield insight into the rate-determining step (phase boundary control or diffusion control). An analysis of the Avrami exponent suggests a phase boundary mechanism.

3.6. Thermodynamic Analysis. Thermodynamic parameters, that is, enthalpy change (ΔH^*/J·mol^{-1}), heat capacity (C_p/J·mol^{-1}·K^{-1}), entropy change (ΔS^*/J·mol^{-1}·K^{-1}), and Gibbs energy change (ΔG^*/J·mol^{-1}) were calculated from the DSC experiment. The enthalpy change was calculated directly from the amount of heat change involved in each step per unit mass of the test sample. ΔH^*, ΔS^*, and ΔG^* were calculated using the following equations:[15,16]

$$C_p = \frac{\Delta H}{\Delta T} \tag{6}$$

$$\Delta S^* = 2.303 C_p \log \frac{T_2}{T_1} \tag{7}$$

$$\Delta G^* = \Delta H^* - T_p \Delta S^* \tag{8}$$

where $\Delta T = T_2 - T_1$, T_1 is the temperature at which the DSC peak begins to depart the baseline, and T_2 is the temperature at which the peak lands. T_p is the DSC peak temperature at the corresponding stage.

The values of ΔH^*, ΔS^*, C_p, and ΔG^* were calculated and found to be 104.64 kJ·mol^{-1}, 72.40 J·K^{-1}·mol^{-1}, 290.75 J·K^{-1}·mol^{-1}, and 744.57 kJ·mol^{-1} for the dehydration reaction and −852.61 kJ·mol^{-1}, −10.74 J·K^{-1}·mol^{-1}, −968.21 J·K^{-1}·mol^{-1}, and 5.77 J·mol^{-1} for a transition form, respectively. The transition phase can be considered as the transformation of an amorphous to a crystalline form of this compound.[7,8] It is well-known that ΔS^* can be less than, equal to, or higher than zero. In the case when $\Delta S^* < 0$, the reactions are classified as "slow" and when $\Delta S^* > 0$ as "fast".[28−30] The positive value of ΔS^* indicates a malleable activated complex that leads to a large number of degrees of freedom of rotation and vibration, whereas the negative value of ΔS^* indicates a highly ordered activated complex, and the degrees of freedom of rotation as well as of vibration are less than they are in the nonactivated complex. Therefore, the dehydration reaction and a transition form of $Al_{0.5}Fe_{0.5}PO_4 \cdot 2.5H_2O$ may be interpreted as "fast" and "slow" stages, respectively.[28−30] The positive and negative values of the enthalpy ΔH^* for the dehydration reaction and a transition form are in good agreement with an endothermic and an exothermic effect in DTA and DSC data, respectively. The positive and negative values of ΔG^* indicate that nonspontaneous and spontaneous processes for dehydration and a transition form stages, respectively. The thermodynamic parameters obtained indicate that the dehydration reaction is softer than the transition phase reaction. The results obtained in this work are different from those of the individual metal phosphates ($AlPO_4 \cdot 2H_2O$[17] and $FePO_4 \cdot 2H_2O$)[18] reported in our previous work.

4. Conclusions

The results obtained in this study show that the dehydration behavior of an $Al_{0.5}Fe_{0.5}PO_4 \cdot 2.5H_2O$ solid solution varies with the function of their cations (Al(III) and Fe(III)). The feature of great interest here is that $Al_{0.5}Fe_{0.5}PO_4 \cdot 2.5H_2O$ decomposes at a relatively low temperature (< 300 °C). A fluctuating value of *E* for different α can be assigned to a complex multistep reaction process, which corresponds to the different interactions of iron and aluminum with water molecules in the skeleton. The thermal behavior and kinetic and thermodynamic parameters of the dehydration reaction of $Al_{0.5}Fe_{0.5}PO_4 \cdot 2.5H_2O$ are different from those of individual metal phosphates ($AlPO_4 \cdot 2H_2O$ and $FePO_4 \cdot 2H_2O$), which result from the perturbation of the molecular orbitals of the anion and cations occurring during the formation of the studied compound. The kinetic and thermodynamic data obtained from such studies can be directly applied in material science for the synthesis of various composite compounds.

Literature Cited

(1) Perri, E.; Tsamouras, D.; Dalas, E. Ferric Phosphate Precipitation in Aqueous Media. *J. Cryst. Growth* **2000**, *213*, 93.
(2) Lindsay, W. L.; Vlek, P. L. G.; Chien, S. H. Phosphate minerals. In *Minerals in soil environment*, 2nd ed.; Dixon, J. B., Weed, S. B., Eds.; Soil Science Society of America: Madison, WI, 1989; pp 1089−1130.

(3) Kniep, R.; Mootz, D.; Vega, A. Variscite. *Acta Crystallogr., Sect. B* **1977**, *33*, 263–265.
(4) Kniep, R.; Mootz, D. Metavariscite: A redetermination of its crystal structure. *Acta Crystallogr., Sect. B* **1973**, *29*, 2292–2294.
(5) Scaccia, S.; Carewska, M.; Prosini, P. P. Thermoanalytical Study of Iron(III) Phosphate obtained by Homogeneous Precipitation from Different Media. *Thermochim. Acta* **2004**, *41*, 381.
(6) Zaghib, K.; Julien, C. M. Structure and Electrochemistry of $FePO_4 \cdot 2H_2O$ Hydrate. *J. Power Sources* **2005**, *142*, 279.
(7) Song, Y.; Zavalij, P. Y.; Suzuki, M.; Whittingham, M. S. New Iron(III) Phosphate Phases: Crystal Structure and Electrochemical and Magnetic Properties. *Inorg. Chem.* **2002**, *41*, 5778.
(8) Scaccia, S.; Carewska, M.; Bartolomeo, A. D.; Prosini, P. P. Thermoanalytical Investigation of Iron Phosphate obtained by Spontaneous Precipitation from Aqueous Solutions. *Thermochim. Acta* **2002**, *383*, 145.
(9) Scaccia, S.; Carewska, M.; Bartolomeo, A. D.; Prosini, P. P. Thermoanalytical Investigation of Nanocrystalline iron(II) Phosphate obtained by Spontaneous Precipitation from Aqueous Solutions. *Thermochim. Acta* **2003**, *397*, 135.
(10) Hsu, P. H. Crystallization of variscite at room temperature. *Soil Sci.* **1982**, *133*, 305–313.
(11) Youssif, M. I.; Mohamedb, F. S.; Aziz, M. S. Chemical and physical properties of $Al_{1-x}Fe_xPO_4$ alloys Part I. Thermal stability, magnetic properties and related electrical conductivity. *Mater. Chem. Phys.* **2004**, *83*, 250–254.
(12) Siva Kumar, V.; Padmasri, A. H.; Satyanarayana, C. V. V.; Ajit Kumar Reddy, I.; David Raju, B.; Rama Rao, K. S. Nature and mode of addition of phosphate precursor in the synthesis of aluminum phosphate and its influence on methanol dehydration to dimethyl ether. *Catal. Commun.* **2006**, *7*, 745–51.
(13) Arjona, A. M.; Alario Franco, M. A. Kinetics of the thermal dehydration of variscite and specific surface area of the solid decomposition products. *J. Therm. Anal.* **1973**, *5*, 319–328.
(14) Stojakovic, D.; Rajic, N.; Sajic, S.; Logar, N. Z.; Kaucic, V. A kinetic study of the thermal degradation of 3-methylaminopropylamine inside $AlPO_4$-21. *J. Therm. Anal. Calorim.* **2007**, *87*, 337–343.
(15) Ŝesták, J. *Thermodynamical properties of solids*; Academia Publishers: Prague, 1984.
(16) Young, D. *Decomposition of Solids*; Pergamon Press: Oxford, 1966.
(17) Boonchom, B.; Danvirutai, C. Kinetics and thermodynamics of thermal decomposition of synthetic $AlPO_4 \cdot 2H_2O$. *J. Therm. Anal. Calorim.* **2009**, *98*, 771–777.
(18) Boonchom, B. Thermodynamics and kinetics of the dehydration reaction of $FePO_4 \cdot 2H_2O$. *Physica B (Amsterdam, Neth.)* **2010**, *405*, 2350−2355.
(19) Frost, R. L.; Weier, M. L. Vibrational Spectroscopy of Natural Augelite. *J. Mol. Struct.* **2004**, *697*, 207.
(20) Breitinger, D. K.; Mohr, J.; Colognesi, D.; Parker, S. F.; Schukow, H.; Schwab, R. G. Vibrational Spectra of Augelites $Al_2(OH)_3(XO_4)$ (X = P, As, V). *J. Mol. Struct.* **2001**, *563*−*564*, 377.
(21) Vyazovkin, S. Computational Aspects of Kinetic Analysis: Part C. The ICTAC Kinetics Project—the light at The End of The Tunnel? *Thermochim. Acta* **2000**, *355*, 155.
(22) Ozawa, T. A New Method of Analyzing Thermogravimetric Data. *Bull. Chem. Soc. Jpn.* **1965**, *38*, 1881.
(23) Kissinger, H. E. Reaction Kinetics in Differential Thermal Analysis. *J. Anal. Chem.* **1957**, *29*, 1702.
(24) Li, Z.; Shen, X.; Feng, X.; Wang, P.; Wu, Z. Non-isothermal kinetics studies on the thermal decomposition of zinc hydroxide carbonate. *Thermochim. Acta* **2005**, *438*, 102–106.
(25) Ioiţescu, A.; Vlase, G.; Vlase, T.; Doca, N. Kinetics of decomposition of different acid calcium phosphates. *J. Therm. Anal. Calorim.* **2007**, *88*, 121–125.
(26) Afify, N. A new method to study the crystallization or chemical reaction kinetics using thermal analysis technique. *J. Phys. Chem. Solids* **2008**, *69*, 1691–1697.
(27) Zhang, Y.; Lv, M.; Chen, D. D.; Wu, J. Q. Leucite Crystallization Kinetics with Kalsilite as a Transition Phase. *Mater. Lett.* **2007**, *61*, 2978–2981.
(28) Vlaev, L. T.; Nikolova, M. M.; Gospodinov, G. G. Non-Isothermal Kinetics of Dehydration of Some Selenite Hexahydrates. *J. Solid State Chem.* **2004**, *177*, 2663.
(29) Vlaev, L.; Nedelchev, N.; Gyurova, K.; Zagorcheva, M. A comparative study of non-isothermal kinetics of decomposition of calcium oxalate monohydrate. *J. Anal. Appl. Pyrolysis* **2008**, *81*, 253–262.
(30) Singh, B. K.; Sharma, R. K.; Garg, B. S. Kinetics and molecular modeling of biologically active glutathione complexes with lead(II) ions. *J. Therm. Anal. Calorim.* **2006**, *84*, 593–600.

Received for review January 29, 2010. Accepted May 16, 2010. This work is financially supported by the Thailand Research Fund (TRF), the Commission on Higher Education (CHE): Research Grant for New Scholar, and the National Nanotechnology Center (NANOTEC) NSTDA, Ministry of Science and Technology, Thailand, through its "Center of Excellence Network" program.

JE100096E